ELSEVIER

Applied Catalysis A: General 167 (1998) 295–308

APPLIED CATALYSIS A: GENERAL

A Rietveld analysis of the transformation of $(La–Sr–V–O)_{reduced}$ to $(La–Sr–V–O)_{oxidized}$ solids and the effect on their surface catalytic properties

Pantelis N. Trikalitis[a], Thomas V. Bakas[b], Aliki C. Moukarika[b], Antonios T. Sdoukos[a], Thomas Angelidis[c], Philip J. Pomonis[a,*]

[a] *Department of Chemistry, University of Ioannina, Ioannina 45332, Greece*
[b] *Department of Physics, University of Ioannina, Ioannina 45332, Greece*
[c] *Department of Chemistry, University of Thessaloniki, Thessaloniki 54006, Greece*

Received 22 July 1997; received in revised form 20 October 1997; accepted 21 October 1997

Abstract

The transformation of the crystal phases of the system $(La–Sr–V–O)_{reduced}$, having the general formula $La_{1-x}Sr_xVO_3$ (x=0.0, 0.05, 0.1, 0.2, 0.4, 0.6, 0.8, 0.9, 0.95, 1.0) and the perovskite structure, towards the $(La–Sr–V–O)_{oxidized}$ one, was studied using the Rietveld analysis. The oxidized system contains the crystal phases $LaVO_4$, $Sr_2V_2O_7$ and $Sr_3V_2O_8$ which originate from the crystal phases $LaVO_3$ and $SrVO_3$ existing in the reduced system. The oxidized solids exhibits surface areas (BET) around 8–10 $m^2\,g^{-1}$ while the reduced ones much lower ~1 $m^2\,g^{-1}$. SEM studies showed that the oxidized particles exhibits a much more irregular surface with pores, cracks, steps and similar features which lack in the reduced solids. The oxidized solids rich in Sr show also a platelet-like structure. The acid/base function of the surface was studied using the isopropanol decomposition as a test reaction towards propene or acetone. The oxidized forms of the solids exhibits stronger acidic properties as compared to the reduced one and lead to dehydration towards propene while the reduced solids exhibit also considerable dehydrogenation activity. The rest features of catalytic action, like reaction rate and apparent activation energies appear rather similar and a common compensation effect, for the reduced and oxidized solids, is observed. The variation of the reaction path towards dehydrogenation or dehydration is related to the intermediate electronegativity of the solids for both the reduced and the oxidized samples. © 1998 Elsevier Science B.V.

Keywords: Perovskite; Rietveld; Isopropanol; Acid–base catalyst

1. Introduction

Binary oxides containing V^{3+} and V^{4+} have been little studied in relation to their surface catalytic properties. In the relevant literature the only such material studied appears to be $SrVO_3$ for the oxidation of benzene and methanol [1] as well as electrode material in anodic oxidations [2]. $LaVO_3$ perovskites have been prepared but not tested as catalysts [3] while binary oxides of vanadium of various structures have been proposed as catalysts for vapour phase dehydrogenation of paraffins [4,5]. Nevertheless binary vana-

*Corresponding author.

PII S0926-860X(97)00324-4

dium oxides and especially $La_{1-x}Sr_xVO_3$ have been extensively studied for their structural, magnetic and conductive properties [6–9]. On the contrary binary oxides containing V^{5+} have been extensively studied in the last years in relation to selective oxidative dehydrogenation of propane [10,11], butane [11] and ethylbenzene [12]. Those studies are mainly concerned with the activity and selectivity of Mg–V–O catalysts where vanadium exists in the form of orthovanadates $Mg_3V_2O_8$, pyrovanadates $Mg_2V_2O_7$ or metavanadates MgV_2O_6 and the main interest of the researchers is to pin-point the crystal phase more active and selective for oxydehydrogenation of organics. In a recent publication [13] the series $La_{1-x}Sr_xVO_3$ was prepared and tested for its catalytic action towards an acid/base catalyzed reaction, the isopropanol decomposition. Although such solids are not particularly acidic the substitution of more acidic La^{3+} by the more basic Sr^{2+} provides some insight into the way the variation of the surface acidity alters the selectivity of the above reaction towards propene or acetone. Besides, the introduction of Sr^{2+} in the sites of La^{3+} results in the transformation of V^{3+} to V^{4+}, but this electronic effect was not reflected on the examined surface reaction [13]. The solids $La_{1-x}Sr_xVO_3$ are unstable in oxidative atmosphere and they are easily transformed into corresponding solids containing V^{5+}. The purpose of this paper is to examine the structural transformation of $(La–Sr–V–O)_{reduced}$ to $(La–Sr–V–O)_{oxidized}$ solids using Rietveld quantitative phase analysis [14–16] for a multicomponent system, to detect which of the crystal phases appears as more active and also how the oxidation of the solids affects their surface acid/base behaviour in relation to isopropanol decomposition.

2. Experimental

2.1. Preparation of La–Sr–V–O solids

In the solids La–Sr–V–O, La was gradually $(1-x)$ substituted by Sr (x) with x=0, 0.05, 0.10, 0.20, 0.40, 0.60, 0.80, 0.90, 0.95 and 1.0. The samples were prepared as follows: Calculated amounts of V_2O_5 in water suspension were reduced by two drops of hydrazine and a black slurry was formed after heating slightly in a water bath. Then the calculated quantities of $La(NO_3)_3.6H_2O$ and $Sr(NO_3)_2$ were dissolved in the parent solution and citric acid was added in amounts equivalent to the moles of metals. The mixture obtained, exhibiting a clear blue colour after heating, was dried carefully at 100°C in a water bath. For the preparation of the oxidized solids, the dried samples were fired slowly and gradually in a tubular silica reactor under air flow of 50 ml/min up to 900°C where they remained for 2 h. (Attention: In two cases where the temperature increment was not so slow and gradual enough some mild explosion of the mixture took place, so the system should be adequately protected). Then for the preparation of the reduced solids, the oxidized ones were heated carefully in a tubular reactor under H_2 stream of 10 ml/min up to 900°C for 6 h with an intermediate grinding. The solids obtained are in Table 1.

2.2. Surface area

The specific surface area (ssa) of the obtained solids was checked by N_2 adsorption at 77 K using the single point method in a SORPTY 1700 apparatus. For the reduced materials the specific surface areas (ssa) were very low (1–2 $m^2\ g^{-1}$) so they were ignored in the estimation of catalytic activity. For the oxidized solids the found ssa are listed in Table 1.

2.3. X-Ray diffraction measurements

The prepared solids were examined for their structure by XRD. The powder method was employed in a SIEMENS system with Cu*Ka* radiation (λ=1.5418). The results obtained were used for the quantitative calculation of the crystal phases according to the Rietveld analysis as described next.

2.4. SEM

The prepared samples were photographed for their morphology in a SEM system (JOEL 840-LINK AN IOS with a Be window). A selection of SEM photograph is shown in Fig. 4.

2.5. Catalytic tests

The catalytic experiments for the prepared samples took place in a bench scale plug flow reactor using the

Table 1
The solids La–Sr–V–O and the corresponding percentage of the crystal phases in their reduced and oxidized form as calculated by Rietveld analysis and the ssa of the oxidized solids

Sample	Reduced form			Oxidized form			
	% $LaVO_3$	% $SrVO_3$	% $Sr_3V_2O_8$	% $LaVO_4$	% $Sr_2V_2O_7$	% $Sr_3V_2O_8$	Surface $m^2\ g^{-1}$
La–V–O	100	0	0	100	0	0	5.84
$La_{0.95}$–$Sr_{0.05}$–V–O	99.5	0.5	0	100	0	0	7.76
$La_{0.9}$–$Sr_{0.1}$–V–O	93.6	6.4	0	93.2	5.2	1.6	7.60
$La_{0.8}$–$Sr_{0.2}$–V–O	86.7	13.3	0	87.8	9.2	3.0	7.97
$La_{0.6}$–$Sr_{0.4}$–V–O	60.6	31.6	7.8	61.7	34.4	3.9	9.89
$La_{0.4}$–$Sr_{0.6}$–V–O	37.0	58.6	4.4	33.9	52.1	14.0	9.67
$La_{0.2}$–$Sr_{0.8}$–V–O	20.0	75.2	4.8	17.3	68.1	14.6	6.04
$La_{0.1}$–$Sr_{0.9}$–V–O	7.6	77.0	15.4	10.4	62.2	27.4	7.84
$La_{0.05}$–$Sr_{0.95}$–V–O	3.0	82.5	14.5	5.2	81.6	13.2	9.95
Sr–V–O	0	80.4	19.6	0	87.8	12.2	2.00

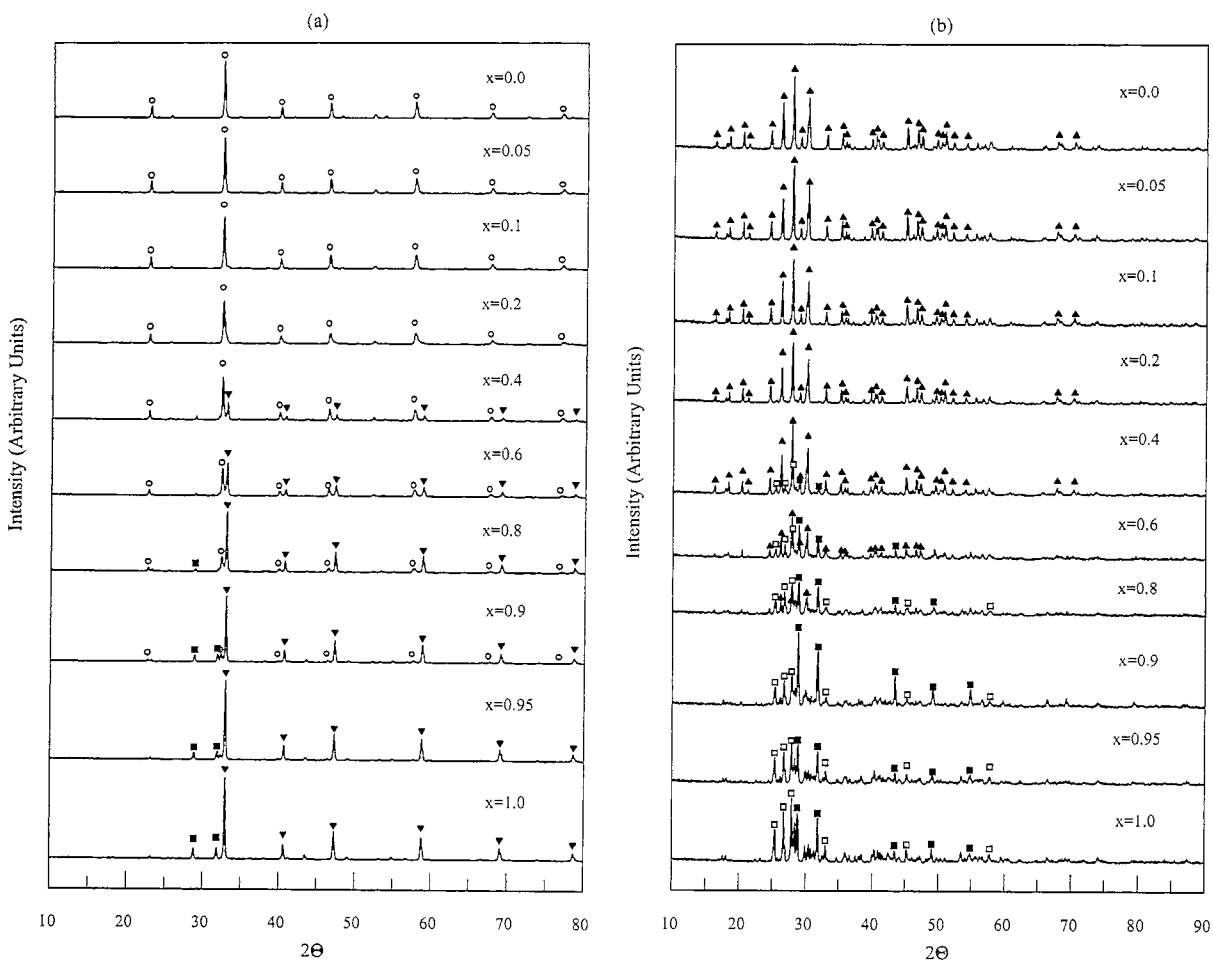

Fig. 1. XRD patterns of solids (a) $(La_{1-x}–Sr_x–V–O)_{reduced}$ and (b) $(La_{1-x}–Sr_x–V–O)_{oxidized}$. (○) $LaVO_3$, (▼) $SrVO_3$, (■) $Sr_3V_2O_8$, (▲) $LaVO_4$, (□) $Sr_2V_2O_7$.

isopropanol decomposition as a probe reaction. The experimental details were similar to those described in Ref. [13]. Briefly the reactor consisted of a silica tube, 1 cm diameter with a perforated glass bed onto which 0.5 g of the catalyst was placed. The system was heated with a tubular furnace controlled by thermocouple equipped with a feed back control-mechanism providing precision >2°C. Analyses of reactants and products were carried out by sampling 1 cm^3 of the gases in a Shimadzu GC-15A Chromatograph equipped with a thermal conductivity detector and connected to Chromatopac C-R6A integrator. The column used for analysis was a 2 m stainless steel 0.125 in. tube (1/8in.) containing 10% Carbovax 20M-Chrom WR/N 0–100 mesh. Helium was used as the carrier gas in the gas chromatograph. Helium flowing (40±2 ml/min) through isopropanol (IPA) saturator drived the alcohol vapours into the reactor at a partial pressure 32.8 mmHg.

3. Results

3.1. XRD data and Rietveld analysis

The XRD data collected are shown in Fig. 1 separately for the $(La–Sr–V–O)_{reduced}$ and the $(La–Sr–V–O)_{oxidized}$ solids.

The identified crystal phases shown in these figures are $LaVO_3$, $SrVO_3$, $Sr_3V_2O_8$, $LaVO_4$ and $Sr_2V_2O_7$ and they actually correspond to the crystal phases identified in similar systems previously [6–9,17,18]. By using as starting models the crystal phases $LaVO_3$ [19], $SrVO_3$ [20] and $Sr_3V_2O_8$ [21] for the reduced

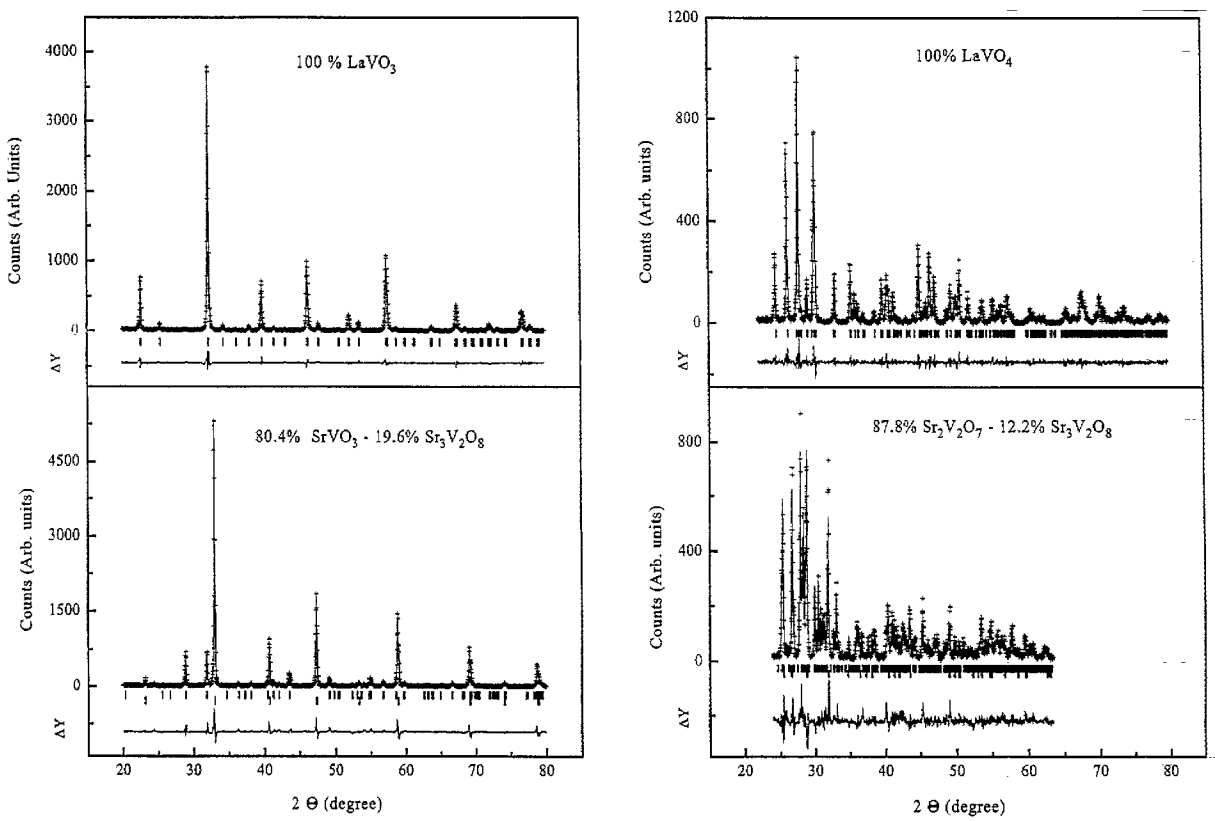

Fig. 2. Results of the Rietveld refinement for the solids indicated and corresponding to the end members of $(La–Sr–V–O)_{reduced}$ and $(La–Sr–V–O)_{oxidized}$ ones.

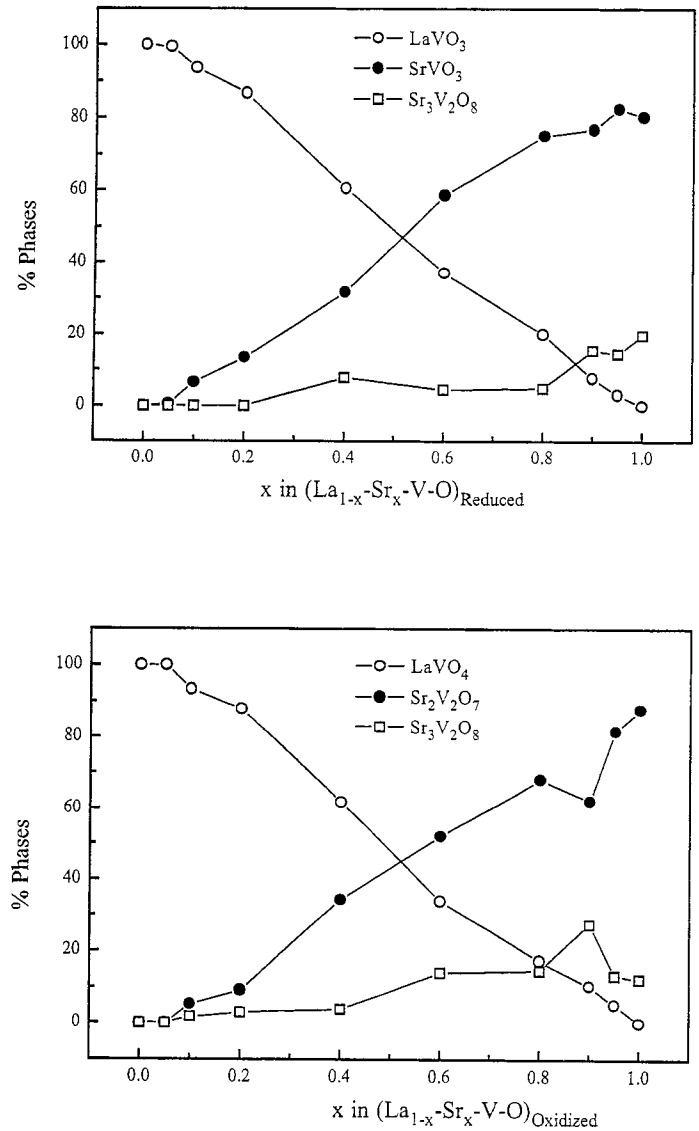

Fig. 3. Percent of the indicated crystal phases according to the Rietveld analysis for the reduced and the oxidized solids as a function of substitution of La by Sr.

solids and $LaVO_4$ [22], $Sr_2V_2O_7$ [23] and $Sr_3V_2O_8$ for the oxidized ones, a Rietveld refinement of the obtained XRD data was made [14–16] using a relevant computer program [24] for quantitative phase analysis of multicomponent mixtures. The following data were used for the refinement of each phase: For the crystal phase $LaVO_3$ the structural parameter of $GdFeO_3$, which is well known as a typical example of orthorhombic destorted perovskite compound ABO_3, were adopted [21]. The crystal phase $SrVO_3$ crystallizes in a cubic perovskite structure, space group P 2_3 [21]. The crystal phase $LaVO_4$ have the Monazite (La, Ce, Y)PO_4 or Huttonite $ThSiO_4$ [22] structure and the structure parameters were taken from a standard reference text book [21]. The structural details of orthovanadate phase $Sr_3V_2O_8$ were taken also from the standard reference text book [21]. The pyrovanadate phase $Sr_2V_2O_7$ has two forms α- and β- which

depend on the annealing temperature. In our case only the α-$Sr_2V_2O_7$ form appears and the corresponding structural details were adopted [23]. The refined parameters accordingly for all the above phases included scale factors, background coefficients, peaks width, profile parameters occupancy factors and cell dimensions and were treated for the Rietveld refinement as described in Ref. [24]. Typical results for two reduced and two oxidized samples are shown in Fig. 2. In this figure the profiles correspond to the end members of

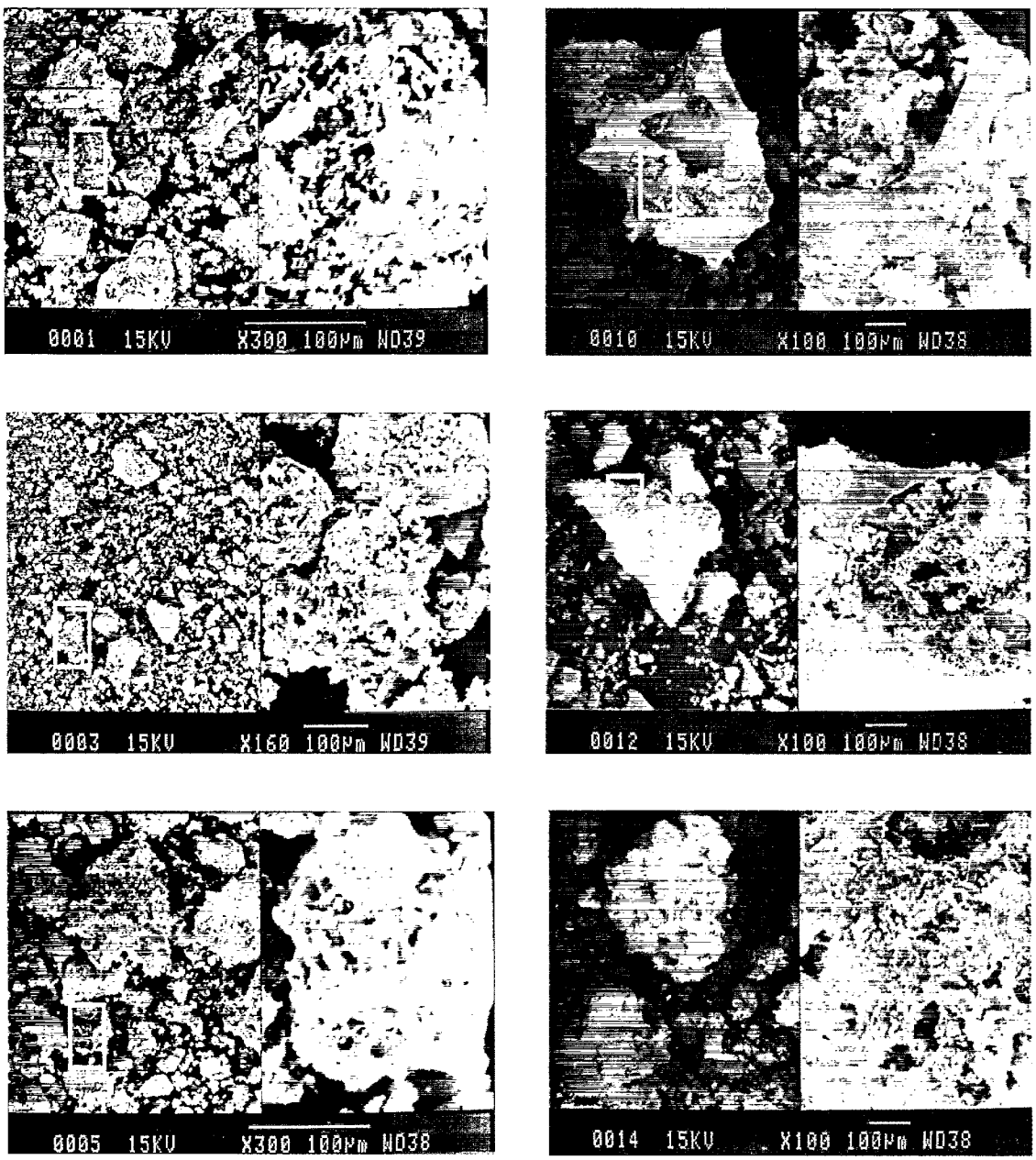

Fig. 4. SEM photographs of typical $(La–Sr–V–O)_{reduced}$ and $(La–Sr–V–O)_{oxidized}$ samples.

the $(La–Sr–V–O)_{reduced}$ and $(La–Sr–V–O)_{oxidized}$ series containing the indicated % of crystal phases as they were found from the optimization of the Rietveld analysis.

In the same figure the satisfactory matching of the experimental with the calculated values of X-ray data can be appreciated from the curve shown at the bottom of each figure which corresponds to the difference between those two quantities. Clearly the discrepancies observed are quite minor and the corresponding crystal phases are noticed in Table 1 and they are plotted as a function of degree of substitution x of La by Sr in Fig. 3.

3.2. SEM

A selection of SEM photograph indicating typical details of the particles is shown in Fig. 4.

A careful observation of them indicates the following typical features of the solids: First, the oxidized materials rich in Sr exhibits a profound platelet-like structure which totally predominates in $(Sr–V–O)_{oxidized}$ solids and disappears at ~50% substitution of Sr by La ($x \approx 0.6–0.4$). This structure is certainly due to the pyrovanadate structure $Sr_2V_2O_7$ as noticed elsewhere [25] and agrees with the XRD data and the Rietveld analysis discussed above. Such a platelet-like structure is also just distinguished in the rich Sr-end member of the reduced series, $SrVO_3$. Second, the surface of the oxidized solids appear much more rugged and tortuous as compared to reduced solids, containing a lot of pores, cracks, steps, foldings and other similar irregularities. It is certainly those extra structural details of the surface which result in the higher specific surface areas of the oxidized samples.

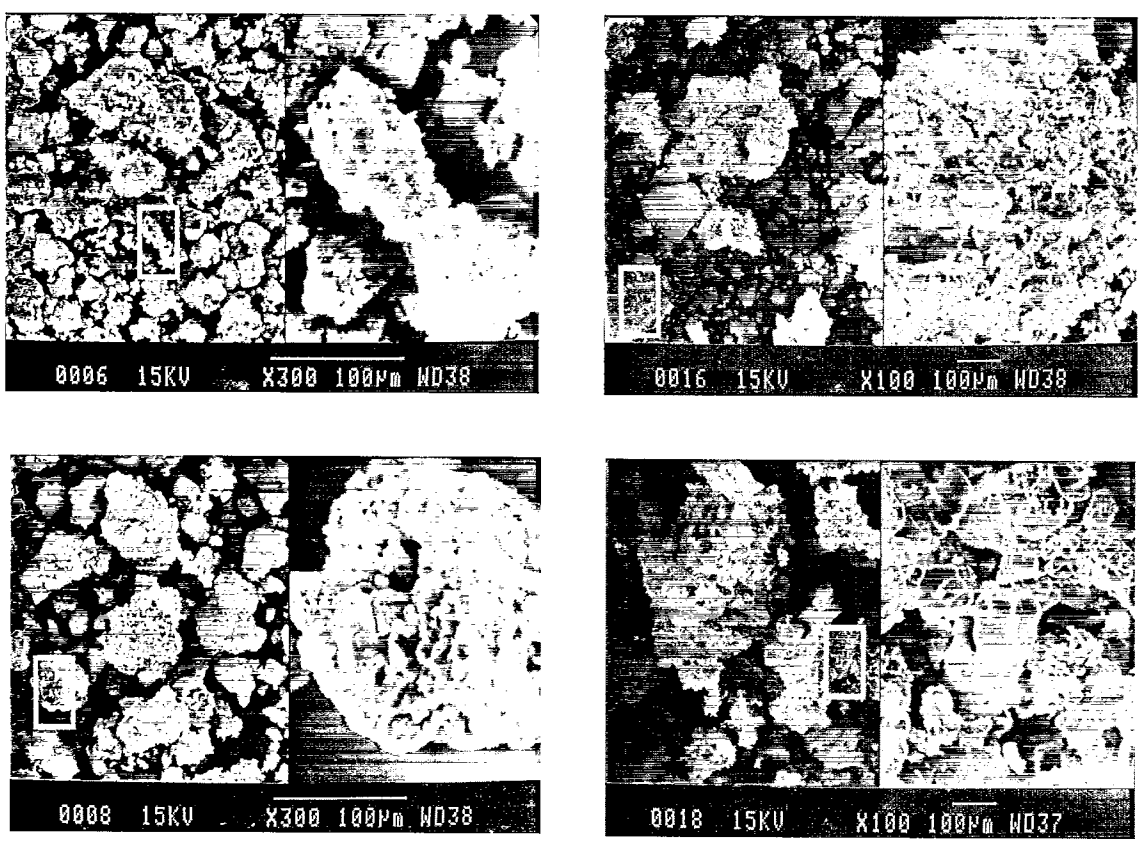

Fig. 4. (continued)

3.3. Catalytic results

In Fig. 5 the catalytic activity of the solids $(La_{1-x}–Sr_x–V–O)_{oxidized}$ for the transformation of isopropanol is given as the reaction rate (mol s^{-1} g^{-1}) versus temperature. In the same figure the selectivity towards propene is given as a function of the conversion. The corresponding rate profiles and selectivities for

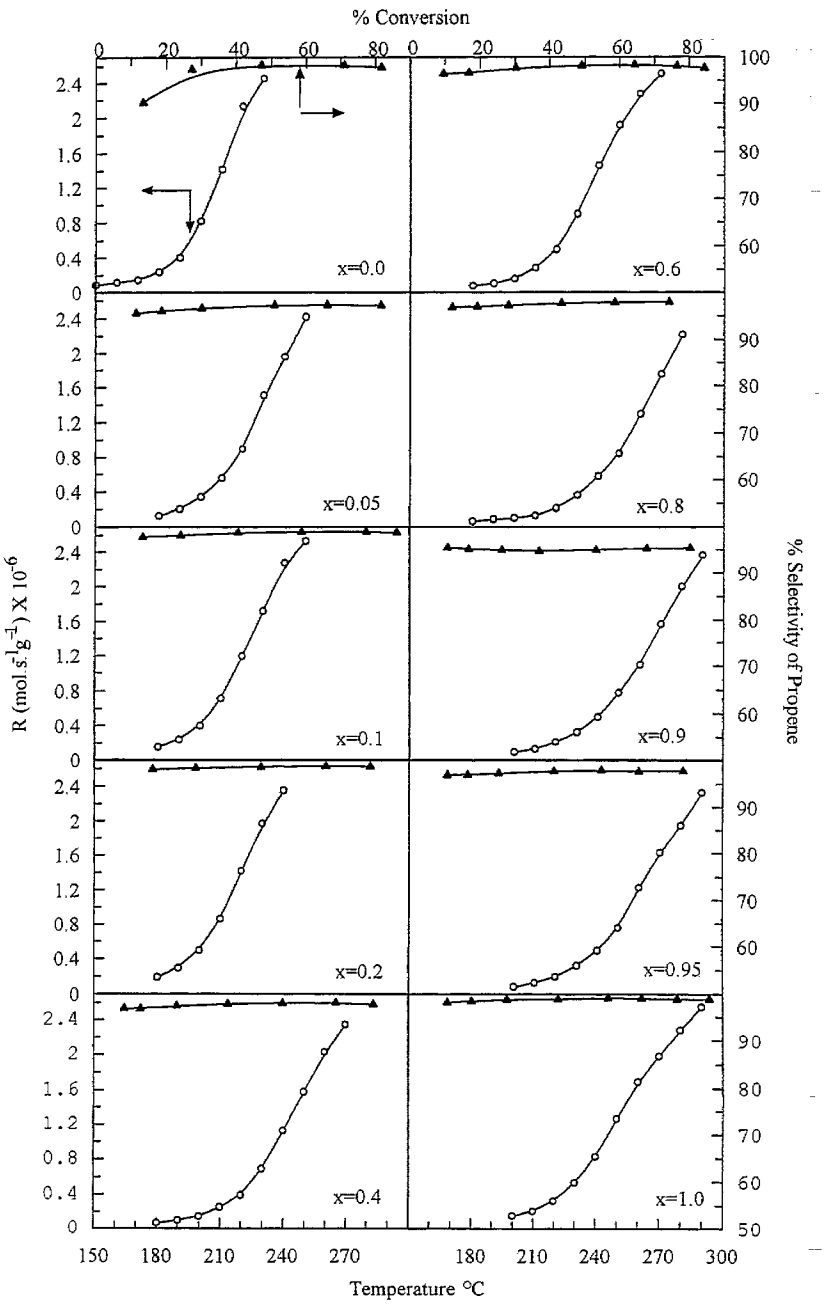

Fig. 5. Rate profiles (○) of isopropanol (mol s^{-1} g^{-1}) versus temperature and the selectivity towards propene versus the degree of conversion (▲) on the solids $(La–Sr–V–O)_{oxidized}$.

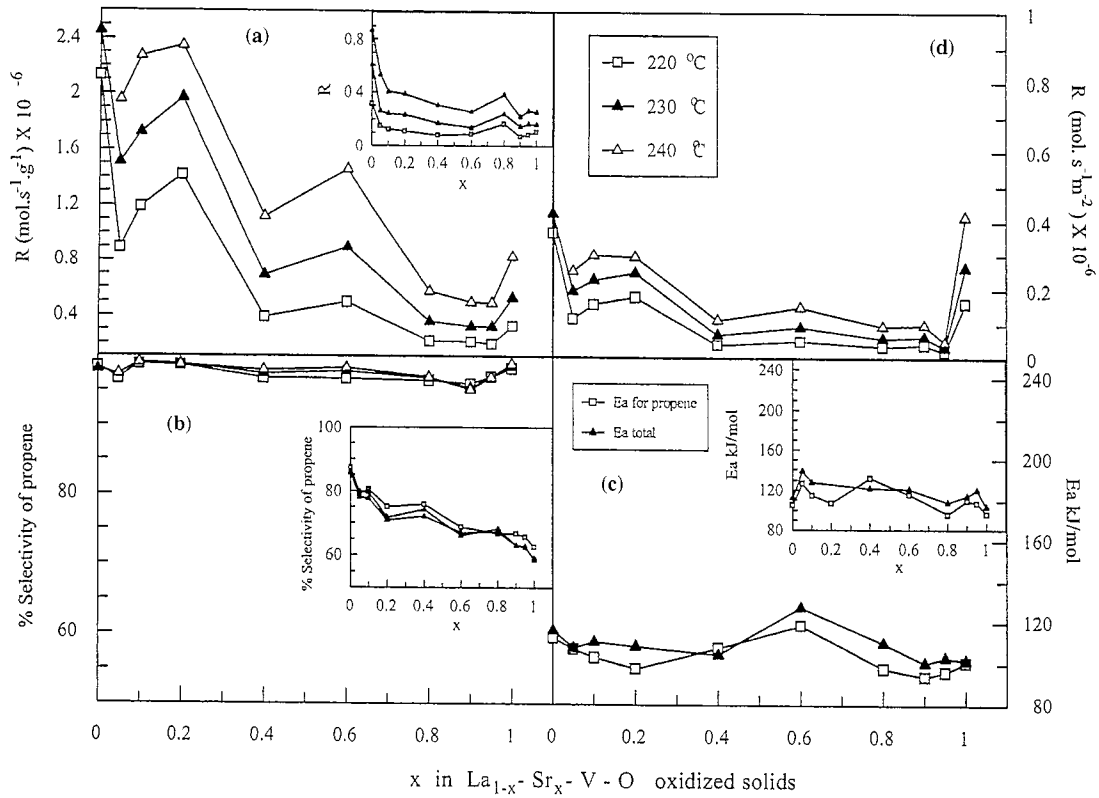

Fig. 6. Reaction rate (mole s^{-1} g^{-1}) of isopropanol (a), selectivity towards propene (b) and apparent activation energies (c) versus the composition of the sample. In the inclusion icons the corresponding values from the reduced solids $La^{3+}_{1-x}Sr^{2+}_{x}V^{3+}_{1-x}V^{4+}_{x}O_3$ are shown from Ref. [13].

the $(La_{1-x}–Sr_x–V–O)_{reduced}$ solids are found in Ref. [13].

In Fig. 6 the reaction rate per g as well per m^2, the selectivity and the calculated apparent activation energies of reaction from the plots log R vs. $1000/T$, are given as a function of degree of substitution (x) of La by Sr for the $(La–Sr–V–O)_{oxidized}$ solids. In the inclusion icons the corresponding values of those quantities for the $(La–Sr–V–O)_{reduced}$ solids (Ref. [13]) are shown for comparison.

4. Discussion

4.1. The transformation of the crystal phases

The analysis of the transformation of the crystal phases of the $(La_{1-x}–Sr_x–V–O)_{reduced}$ solids to $(La_{1-x}–Sr_x–V–O)_{oxidized}$ ones (Fig. 1(a) and (b)) according to the Rietveld standard procedure indicates that the fitting achieved was satisfactory (Fig. 2) and that the discrepancies observed, as shown by ΔY values at the bottom of these figures, are within the experimental errors usually observed in such cases. Furthermore it seems that there is almost an one-to-one transformation of the crystal phases $LaVO_3$ and $SrVO_3$, traced in the $(La_{1-x}–Sr_x–V–O)_{reduced}$ solids, towards the crystal phases $LaVO_4$ and $Sr_2V_2O_7$ observed in the $(La_{1-x}–Sr_x–V–O)_{oxidized}$ ones as shown graphically in Fig. 7.

The % of the third crystal phase $Sr_3V_2O_8$, traced in both cases, is lower but appreciable, reaching values as high as 10%–20% for high Sr content and in one case, $[(La_{0.1}–Sr_{0.9}–V–O)_{oxidized}$ sample], reaches 27.4%.

The transformation of the $LaVO_3$ and $SrVO_3$ reduced crystal phases to the $LaVO_4$ and $Sr_2V_2O_7$

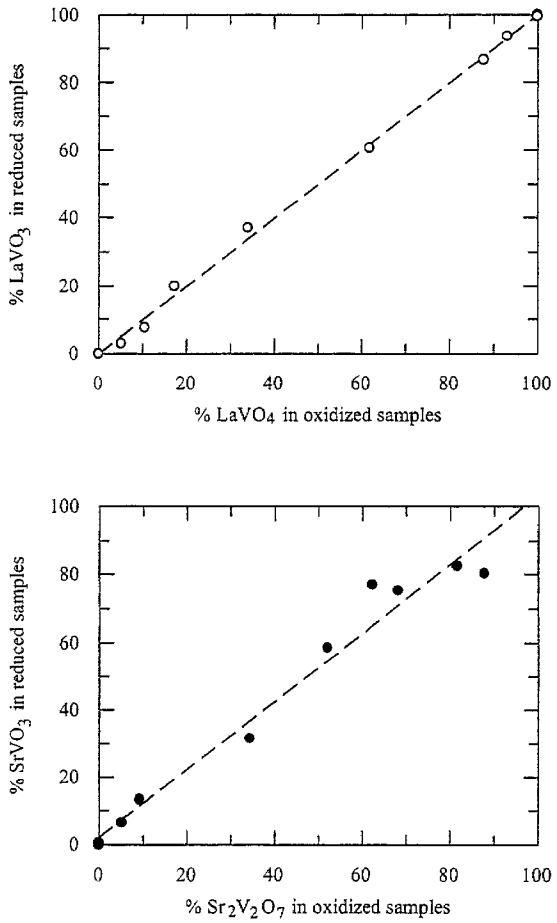

Fig. 7. Transformation of the % crystal phases $LaVO_3$ and $SrVO_3$ in the reduced solids to the % crystal phases $LaVO_4$ and $Sr_2V_2O_7$ traced in the oxidized samples.

oxidized ones has as a direct effect to the increment of the specific surface area of the samples from 1–2 $m^2\,g^{-1}$ to 5–10 $m^2\,g^{-1}$ (Table 1), depending on the composition. There is no any apparent correlation between such an increase with the composition of the solids. Nevertheless it seems that the oxidation process acts against the sintering effects observed during the reduction of solids by H_2. Clearly the surface energy needed to increase the surface of the $(La_{1-x}–Sr_x–V–O)_{reduced}$ solids by one order of magnitude (from 1 to about 10 m^2) should be balanced by the energy supplied to the system by the formation of extra M–O bonds, especially the extra V–O ones.

Let us try to be more specific at this point. Each g of $(La_{1-x}–Sr_x–V–O)_{reduced}$ solids has a ssa around 1 m^2 or 10^{20} $Å^2$. Now each vanadium atom, coordinated via oxygen to neighbouring M (M=Sr, La) atoms corresponds to area $\pi R^2_{V–O–M}$ which equals around ~30–35 $Å^2$. Therefore in the external surface of the reduced solids there exist around $\sim 3\times10^{18}$ V^{3+}–O units. For the $(La_{1-x}–Sr_x–V–O)_{oxidized}$ solids with ssa ~10 $m^2\,g^{-1}$ we have for each g 10^{21} $Å^2$ and in the corresponding external surface area there exist around $\sim 3\times10^{19}$ V^{5+}-O units. So the process of oxidation, leading to the increasing of the ssa, resulted in the creation of $\sim 3\times10^{19}$ V^{5+}–O bonds which are much more thermodynamically stable compared to $\sim 3\times10^{18}$ V^{3+}–O bonds existing on the surface of the reduced particles. The extent of stabilization of the surface brought upon oxidation can be estimated for the system $LaVO_3$–$LaVO_4$ for which $(-\Delta H^0_f)_{LaVO_3} = 1563.4$ kJ/mol and $(-\Delta H^0_f)_{LaVO_4} = 1825.5$ kJ/mol [26]. Therefore upon oxidation there is a stabilization equal to:

$$\delta(-\Delta H^0_f) = (-\Delta H^0_f)_{LaVO_4} - (-\Delta H^0_f)_{LaVO_3} = 262.1\,\text{kJ/mol}$$

From this value we can easily calculate,

$$262.1\times10^3(\text{J/mol}) \times \frac{10^7(\text{ergs/J})}{6.023\times10^{23}(\text{V–O bonds/mol})}4.35 \times 10^{-14}\ \text{ergs/V–O bond}$$

Now since the bonds contributing to the stabilization of the external surface are around $\sim 3\times10^{19}/10$ m^2, the total stabilization should be

$$\delta(-\Delta H^0_f)_{\text{surface V–O bonds}} = 4.35\times10^{-14}\left(\frac{\text{ergs}}{\text{V–O bond}}\right) \times 3\times10^{19}(\text{V–O surface bonds}/10\,m^2) = 13\times10^5\,\text{ergs}/10\,m^2 \approx 13\,\text{ergs/cm}^2$$

This result is in the range of surface energy observed for oxides [27]. Given the rather rough assumptions made for these calculations, the result can be considered certainly in the correct order of magnitude and indicative of the reasons leading to the increase of the surface area upon oxidation. Similar calculations can be carried out not only for the system $LaVO_3$–$LaVO_4$ but also for the solids with Sr-containing crystal phases $SrVO_3/Sr_2V_2O_7/Sr_3V_2O_8$.

An observation can be made at this point relevant to the penetration of the oxidation front and the increase

of the pores, cracks, steps etc in the oxidized samples. The system "equilibrates" its disintegration process in the limit where the energy supplied to the surface of the solid because of the formation of new V^{3+}–O→V^{5+}–O bonds balances the intrinsic surface energy of the solid. Any excess of disintegration to more minute structural details is clearly a waste of energy and avoided according to well known reasons [28]. Such a process might be compared to the distance where the oxidation front ("fire"), started at the external surface of the large reduced particles ("forest"), can travel at least half of their size, up to the center of the particle, oxidizing ("burning") in its way all the reduced vanadium atoms ("trees") to V^{5+} atoms ("ash"). The problem is similar to the typical percolation paradigm [29]. The oxidation front proceeds forming an oxidized percolation cluster which is "disintegrated" and create a lot of novel surface details, which result in the increase of the surface.

4.2. *The effect on the surface catalytic properties*

The main characteristics of the catalytic transformation of isopropanol, as depicted in Fig. 6, include the reaction rate both per g and m^2 of the solids, the selectivity towards propene or acetone as well as the calculated activation energies. In Fig. 8 the observed compensation effect is shown common for both the reduced and the oxidized solids. The catalytic results

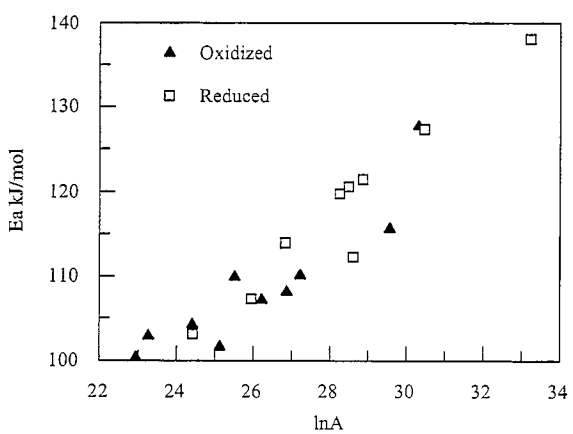

Fig. 8. Compensation effect for the isopropanol decomposition on La–Sr–V–O solids. (□) reduced solids $[La^{3+}_{1-x}Sr^{2+}_{x}V^{3+}_{1-x}V^{4+}_{x}O_3]$ ([13]) and (▲) oxidized solids.

for the $(La–Sr–V–O)_{reduced}$ solids have been taken from Ref. [13] for comparison.

We observed that the reaction rate (mole g^{-1} s^{-1}) on the $(La–Sr–V–O)_{oxidized}$ solids is higher as compared to reduced samples, a fact reflecting the higher surface area of the former. But if the reaction rate is calculated per m^2 for the oxidized solids, then this is found almost similar to the one observed on the reduced solids. No effect of substitution of La by Sr is observed in the whole range of it.

The selectivity towards propene appears almost 100% for the whole range of substitution on the oxidized solids. On the reduced samples it shows a linear drop with increase of Sr-content, which leads to increase of the V^{4+} configuration. These samples show increased dehydrogenating action.

The activation energies, calculated from plots log-$R=f(1000/T)$, are in the same range of magnitude for the oxidized and reduced solids, but the $E_{apparent}$ values observed on the oxidized solids are around ~20 kJ/mol smaller as compared to the reduced solids. An important question now is related to the factors which control the selectivity of the catalysts towards dehydration or dehydrogenation.

In a previous publication referred to the reduced samples[13] the increased production of acetone at high Sr-content was related to the existence of more basic sites on the solids which are the active centers for dehydrogenation [30–34]. But on the oxidized solids this basic effect of Sr-sites is totally lost and only the acid function of the surface towards dehydration prevails. Let us try to quantify the basicity/acidity of the surface for all of our solids using the parameter a which was proposed by Smith [35] as a characteristic of the acidity or basicity of the binary oxides ABO_x. Oxides with $a<-5$ are purely basic, oxides with $0>a>-5$ are amphoteric while for acidic oxides $a>0$. We recall from Ref. [35] that for a reaction

$$AO_y + BO_z \rightarrow ABO_x (y+z=x)$$

the a values are calculated via the relationship

$$[a(AO_y) - a(BO_z)]^2 = -(\Delta H^0_f)_{ABO_x}\ \text{kJ/mol}$$

So if the a values for the simple oxides V_2O_3, VO_2, V_2O_5, La_2O_3 and SrO are known we can easily calculate the a values for the $(La–Sr–V–O)_{reduced}$ and $(La–Sr–V–O)_{oxidized}$ solids, taking into account the % of each crystal phase as found by the Rietveld

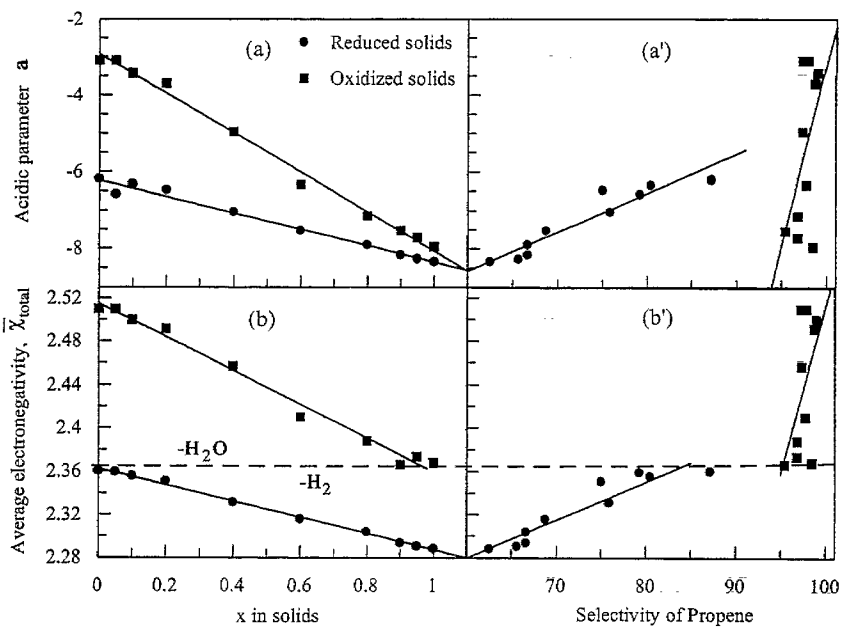

Fig. 9. (a) Mean values of the acidic parameter a of the oxidized and reduced (La–Sr–V–O) solids as a function of their composition, taking into account the contribution of every crystal phase identified according to the Rietveld analysis and (a′) its relationship with selectivity. (b) The average electronegativity of the solids taking into account the contribution of each indentified crystal phase and (b′) its relation with selectivity.

analysis. Using the data from Ref. [35] and the same treatment as in Ref. [13] we can easily estimate the a values for the binary oxides traced in our solids, which are as follows: $Sr_3V_2O_8$, $a=-8.4$; $SrVO_3$, $a=-8.32$; $Sr_2V_2O_7$, $a=-7.9$; $LaVO_3$, $a=-6.2$; $LaVO_4$, $a=-3.1$. Then the a values for their mixture, as this was identified from the Rietveld analysis, have been calculated and plotted versus x in Fig. 9(a) and versus the selectivity in Fig. 9(a′).

From these figures we observe two particular points: First, for the reduced ABO_3 solids in the whole range of substitution of La by Sr the a values are smaller than -5 indicating that such solids are purely basic according to the methodology and terminology of Smith [35]. This result is in line with the observations made by Busca and co-workers [36–38] who based mainly on IR studies concluded that such perovskite materials are predominantly of basic character. The corresponding oxidized solids and especially the ones with high content of Sr appear also basic ($a<-5$) while those with high La content appear as amphoteric $0>a>-5$ (see Fig. 9(a)). The second observation is that although the mean a values for the oxidized solids for $x\geq 0.6$–0.7 is lower than the a values for the reduced samples, no dehydrogenation activity is observed for the former as observed for the later (see selectivities plot in Fig. 9(a′). In other words the mean values of a of the solids is not a critical factor controlling the dehydration or the dehydrogenation routes.

In a second approach let us adopt the mean electronegativity method of Sanderson [39–42]. Then selecting the χ values for the relevant elements from a standard electronegativity scale like that of Allred [43], we can find out the average $\overline{\chi}$ values for the crystal phases which make up our solids. Such $\overline{\chi}$ values are as follows: $LaVO_3$, $\overline{\chi}=2.36$; $SrVO_3$, $\overline{\chi}=2.29$; $LaVO_4$, $\overline{\chi}=2.51$; $Sr_2V_2O_7$, $\overline{\chi}=2.38$ and $Sr_3V_2O_8$, $\overline{\chi}=2.28$. From those values the mean total Sanderson electronegativity of the solids $\overline{\chi}_{total}$ have been calculated, taking into account the contribution of each crystal phase from Table 1. The results are plotted in Fig. 9(b) versus x and versus the selectivity in Fig. 9(b′). We can see from this figure that the total electronegativity $\overline{\chi}_{total}$ values control selectivity in a uniform way for both the reduced and the oxidized

solids. In other words the dehydrogenation activity in our solids appears for $\overline{\chi}_{total}$ values below ~2.37 while above this value only dehydration appears.

An alternative explanation for the selectivity on our solids has probably to do with the hiding of the Sr atoms from the surface of the oxidized solids because of crystallographic reasons. Indeed it has been observed in the past [36,37] that perovskite oxides of the form ABO_3 are less acidic compared to the corresponding spinels AB_2O_4 or the pyro- and ortho-corresponding oxides $A_2B_2O_7$ and $A_3B_2O_8$ because of different crystallographic structure. Namely in the structure ABO_3 the B cations (V^{3+} and/or V^{4+} in our case) are compressed to the interior of the solids [36,37]. Therefore the A cations, including Sr^{2+} in our case, are more exposed and their basic action towards dehydrogenation becomes apparent. On the contrary in structures like $A_2B_2O_7$ and/or $A_3B_2O_8$ both A and B cations are equally exposed on the surface which appear to act in a more acidic way. Now since the structure $Sr_3V_2O_8$ exist both in oxidized and reduced solids and the structures $LaVO_3$ and $LaVO_4$ do not actually show dehydrogenation activity, the differentiation can be pin-pointed to the basic action of $SrVO_3$ solids while its equivalent phase $Sr_2V_2O_7$ does not behave similarly-the basic activity of Sr atoms is lost for crystallographic/geometrical reasons.

5. Conclusions

The system (La_{1-x}–Sr_x–V–O) with x=0.0, 0.05, 0.1, 0.2, 0.4, 0.6, 0.8, 0.9, 0.95, 1.0) can be either stabilized in an oxidized or reduced form under relevant heating conditions. XRD and Rietveld analysis shows that the reduced form contains the crystal phases $LaVO_3$ and $SrVO_3$ (depending on composition) as well as $Sr_3V_2O_8$ to a smaller percentage. The oxidized form contains the crystal phases $LaVO_4$ and $Sr_2V_2O_7$ originated from the corresponding ones of the reduced solids, as well as some $Sr_3V_2O_8$. The oxidized solids rich in Sr showed a platelet-like structure most probably due to the $Sr_2V_2O_7$ phase. All the oxidized solids possess a more rugged and tortuous external surface (8–10 $m^2\,g^{-1}$) as compared to the reduced one for which their external surface (~1 $m^2\,g^{-1}$) is more regular. The catalytic behaviour of those solids for the isopropanol decomposition proceeds almost ~100% towards propene on the oxidized solids but 85–60% towards propene on the reduced solids, the rest being acetone. Although this increased acid action of the oxidized materials towards dehydration is attributed to the action of acidic active center V^{5+}–O existing on their surface while the dehydrogenation activity of Sr basic centers is lost in the oxidized solids. This change in the reaction path is related to a collective property of the solids, namely their mean electronegativity. Alternatively can be attributed to Sr cations which are exposed on the surface of $SrVO_3$ but are less exposed on the oxidized forms $Sr_2V_2O_7$ and $Sr_3V_2O_8$ of the solids.

Acknowledgements

We wish to thank Dr E. Paulidou, SEM unit, University of Thessaloniki, for her help.

References

[1] K.S. De, M.R. Balasubramanian, J. Catal. 81 (1983) 482.
[2] Y. Matsumoto, H. Yoneyama, H. Tamura, J. Electroanal. Chem. 79 (1977) 319.
[3] J.M.D. Tascon, S. Mendioroz, L.G. Tejuca, Z. Phys. Chem., N.F. 124 (1981) 109.
[4] A.T. Guttmann, J.F. Brazdil, P.K. Grasselli, US Patent, 4, 816, 243, 1989.
[5] M.R. Balasubramanian, J. Indian Chem. Soc. 64 (1978) 453.
[6] B. Reuter, M. Vollnik, Naturwissenschaften 50 (1963) 569.
[7] R.G. Egdell, M.R. Harrison, M.D. Hill, L. Porte, G. Wall, J. Phys. C: Solid State Phys. 17 (1984) 2889.
[8] P. Dougier, A. Casalot, J. Solid State Chem. 2 (1970) 346.
[9] P. Dougier, P. Hagenmuller, J. Solid State Chem. 15 (1975) 158.
[10] M.C. Kung, H.H. Kung, J. Catal. 134 (1992) 668.
[11] X. Gao, P. Ruiz, Q. Xin, X. Guo, B. Delmon, J. Catal. 148 (1994) 56.
[12] W.S. Chang, Y.S. Chen, B.L. Yang, Appl. Catal. A: General 124 (1995) 221.
[13] P.N. Trikalitis, P.J. Pomonis, Appl. Catal. A: General 131 (1995) 309.
[14] H.M. Rietveld, Acta Cryst. 22 (1967) 151.
[15] H.M. Rietveld, J. Appl. Cryst. 2 (1969) 65.
[16] D.B. Wiles, R.A. Young, J. Appl. Cryst. 14 (1981) 149.
[17] N. Suzuki, T. Noritake, N. Yamamoto, T. Hioki, Mat. Res. Bull. 26 (1991) 1.
[18] M. Itoh, M. Shikano, R. Liang, H. Kawaji, T. Nakamura, J. Solid State Chem. 88 (1990) 597.

[19] H.C. Nguyen, J.B. Goudenough, Phys. Rev. B 52 (1995) 324.
[20] M.J. Rey, PH. Dehaudt, J.C. Joubert, B. Lambert-Andron, M. Cyrot, F. Cyrot-Lackermann, J. Solid State Chem. 86 (1990) 101.
[21] Ralph W.G. Wyckoff, Grystal Structures, Vol. 3.
[22] T. Nakamura, G. Petzow, L.G. Gauckler, Mat. Res. Bull. 14 (1979) 649.
[23] J. Huang, A.W. Sleight, Mat. Res. Bull. 27 (1992) 581.
[24] D.L. Bish, S.A. Howard, J. Appl. Cryst. 21 (1988) 86.
[25] J. Garcia-Jaca, J.L. Pizaro, J.I.R. Larramendi, L. Lezama, M.I. Arriortua, T. Rojo, J. Mater. Chem. 5(2) (1995) 277–283.
[26] K. Kitayama, D. Zoshima, T. Katsura, Bull. Chem. Soc. Jpn. 56(3) (1983) 689–694.
[27] G. Somorjai, Introduction to Surface Chemistry and Catalysis, chap. 2, Wiley, New York-Chichester-Brisbane-Toronto-Singapore, 1994.
[28] According to William of Ockham (1300–1349) beings must not be multiplied unnecessarily. This tenet known as Ockham's razor, is taken to mean that an explanation should always be made on the fewer possible assumptions or unknows and the fewer of these the more likely the theory is to be correct.
[29] D. Stauffer, A. Aharony, Introduction to Percolation Theory, 2nd ed., Taylor and Francis, London-Washington DC, 1992.
[30] C. Ancion, G. Poncelet, Appl. Catal. A: General 108 (1994) 31.
[31] J.C. Luy, J.M. Parera, Appl. Catal. 13 (1984) 39.
[32] H. Niyama, E. Echigaya, Bull. Chem. Soc. Jpn. 44 (1971) 1739.
[33] L. Nondek, Sedlacek, J. Catal. 40 (1975) 34.
[34] K. Tomke, Z. Phys. Chem., N.F. 106 (1977) 225.
[35] D.W. Smith, J. Chem. Educ. 64 (1987) 480.
[36] G. Busca, V. Buscaglia, M. Leoni, P. Nanni, Chem. Mat. 6 (1994) 955.
[37] M. Daturi, G. Busca, R. Willey, Chem. Mat. 7 (1995) 2115.
[38] J.M.G. Amores, V.S. Escribano, M. Daturi, G. Busca, J. Mat. Chem. 6 (1996) 879.
[39] R.T. Sanderson, Chemical Periodicity, Reinhold, New York, 1960.
[40] K.I. Tanaka, A. Ozaki, J. Catal. 8 (1967) 1.
[41] A. Gervasini, A. Auroux, J. Catal. 131 (1991) 190.
[42] A. Auroux, A. Gervasini, J. Phys. Chem. 94 (1990) 6317.
[43] A. L Allred, J. Inorg. Chem. 17 (1961) 215.